The EMBO Journal vol.15 no.12 pp.3164–3173, 1996

The structure and function of the replication terminator protein of *Bacillus subtilis*: identification of the 'winged helix' DNA-binding domain

Karnire S.Pai, Dirksen E.Bussiere, Fenggang Wang[1], Clyde A.Hutchison III[1], Stephen W.White and Deepak Bastia[2]

Department of Microbiology, Duke University Medical Center, Durham, NC 27710 and [1]Department of Microbiology, University of North Carolina, Chapel Hill, NC 27599, USA

[2]Corresponding author

The replication terminator protein (RTP) of *Bacillus subtilis* impedes replication fork movement in a polar mode upon binding as two interacting dimers to each of the replication termini. The mode of interaction of RTP with the terminus DNA is of considerable mechanistic significance because the DNA–protein complex not only localizes the helicase-blocking activity to the terminus, but also generates functional asymmetry from structurally symmetric protein dimers. The functional asymmetry is manifested in the polar impedance of replication fork movement. Although the crystal structure of the apoprotein has been solved, hitherto there was no direct evidence as to which parts of RTP were in contact with the replication terminus. Here we have used a variety of approaches, including saturation mutagenesis, genetic selection for DNA-binding mutants, photo cross-linking, biochemical and functional characterizations of the mutant proteins, and X-ray crystallography, to identify the regions of RTP that are either in direct contact with or are located within 11 Å of the replication terminus. The data show that the unstructured N-terminal arm, the α3 helix and the β2 strand are involved in DNA binding. The mapping of amino acids of RTP in contact with DNA confirms a 'winged helix' DNA-binding motif.

Keywords: DNA–protein interaction/replication termination

Introduction

Termination of DNA replication in most prokaryotes occurs at specific replication termini (Kuempel *et al.*, 1977; Louarn *et al.*, 1977; Kolter and Helinski, 1978; Bastia *et al.*, 1981; Lewis *et al.*, 1990; Carrigan *et al.*, 1991). In *Escherichia coli* and *Bacillus subtilis*, the process is mediated by the interaction of the replication terminator proteins with the sequence-specific replication termini (Hill *et al.*, 1989; Sista *et al.*, 1989; Lewis *et al.*, 1990; Kaul *et al.*, 1994; Sahoo *et al.*, 1995a,b). The protein–DNA complex at the terminus imposes a polar block to the DNA unwinding activity of the replicative helicase operating ahead of the replication fork (Khatri *et al.*, 1989; Lee *et al.*, 1989; Hiasa and Marians, 1992; Kaul *et al.*, 1994; Sahoo *et al.*, 1995a,b). We have adopted the term 'contrahelicase' to describe this novel property (Khatri *et al.*, 1989). The polarity is believed to be determined by the topology of the protein–DNA interaction of the terminator protein with the terminus DNA (Khatri *et al.*, 1989; Sahoo *et al.*, 1995a).

Much of the *in vivo* analysis of the replication terminus of *B.subtilis* has been carried out by Wake and co-workers (Lewis and Wake, 1989; Lewis *et al.*, 1989, 1990; Carrigan *et al.*, 1991; Smith and Wake, 1992; Young and Wake, 1994). The replication terminator protein (RTP) of *B.subtilis* has a subunit mol. wt of 14 500 and functions as a dimer (Lewis *et al.*, 1990). A monomer of RTP has four α-helices, three β-strands and an N-terminal unstructured arm, as depicted in Figure 1A (Bussiere *et al.*, 1995). The replication terminus comprises a core binding site and an overlapping auxiliary site, as shown in Figure 1B (Carrigan *et al.*, 1991; Langley *et al.*, 1993; Sahoo *et al.*, 1995a). A dimer of RTP first binds to the core site, and this promotes the binding of a second dimer to the auxiliary site by cooperative protein–protein interactions (Carrigan *et al.*, 1991; Smith and Wake, 1992). A single dimer of RTP bound to the core site is ineffective in eliciting contrahelicase activity and causing fork arrest both *in vivo* (Lewis *et al.*, 1990) and *in vitro* (Sahoo *et al.*, 1995a). We have recently solved the crystal structure of the replication terminator apoprotein of *B.subtilis* at 2.6 Å (Bussiere *et al.*, 1995). The crystal structure, together with pertinent biochemical data on the nature of the cognate DNA sequence, suggested a model for the RTP–DNA interaction. A pair of dimer-related α-helices (α3) and β-ribbons (strands β2/β3 and the connecting loop) could make contacts with two successive major and the minor grooves of the DNA, respectively.

Here we describe a series of genetic and biochemical experiments both to support and enhance this model. A genetic selection scheme was used to test the DNA-binding properties of RTP mutants that were generated either from a library or from random mutagenesis. This approach was adopted to reveal amino acids that might contact DNA unbiased by our modeling studies. Using gel mobility shift assays and photochemical cross-linking, we have further characterized the various regions of RTP that contact with DNA. Finally, because impairment of function by mutagenesis can also be caused by changes in protein structure, these results have been carefully analyzed by computer graphics and, in one case, by X-ray crystallography. Overall, the results fully support our model and are consistent with RTP being a member of the 'winged helix' family of DNA-binding proteins, as suggested by Swindells (1995). In addition, they confirm that the N-terminal arm of the protein which is unstructured in the crystal structure is a crucial DNA-binding element of RTP. Finally, biochemical analyses of the mutant

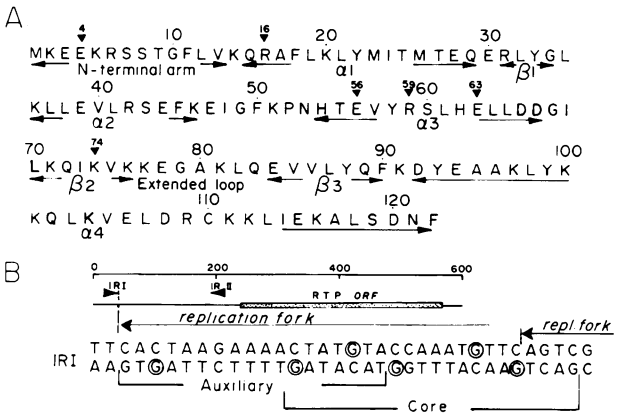

Fig. 1. The primary structure of the replication terminator protein (RTP) and of the replication terminus (IRI or BS3) of *B.subtilis*. (**A**) The amino acid sequence and features of the secondary structure of RTP. Note the location of the four α-helices, the three β-strands and the extended loop between β2 and β3. (**B**) The replication termini IRI and IRII and the region encoding RTP. An expanded view of IRI is shown. Note the overlapping core and the auxiliary sites and the G residues (circled) that make contact with RTP.

forms of the protein confirm that the magnitude of the contrahelicase activity in most cases directly correlated with the avidity of binding. An exception to this general pattern is a mutant located in the β2 region that did not show any detectable loss of DNA binding, but suffered a moderate loss of contrahelicase activity and a complete loss of the ability to arrest replication forks *in vitro*.

Results

Chemical mutagenesis, oligo-directed saturation mutagenesis and selection for mutants defective in DNA binding

Initially, we wished to determine the regions of RTP that may be involved in DNA binding, independent of the predictions made by the crystal structure of the RTP apoprotein. The basic approach was to mutagenize the *rtp* gene and then to genetically select for DNA-binding mutants using a scheme developed by Elledge *et al.* (1989). The principle behind the selection scheme is shown in Figure 2. Briefly, the expression of the reporter gene encoding spectinomycin resistance (*aadA*) is suppressed by an antisense transcript emanating from the Preg promoter (Figure 2A). Insertion of the replication terminus BS3 (IRI) of *B.subtilis* between the promoter and the reporter gene at the indicated site (Figure 2B) blocks the synthesis of the antisense RNA when the normal RTP is present in the cell milieu. The binding of RTP to the BS3 site functionally mimics a repressor–operator complex that blocks the synthesis of the antisense RNA, thus allowing the expression of spectinomycin resistance (Sp^r). The absence of RTP or a mutation in RTP that reduces DNA binding to BS3 *in vivo* results in spectinomycin sensitivity (Sp^s).

The first approach was chemical mutagenesis and the second employed a series of synthetic, overlapping oligonuclotides (Table I) that were synthesized in such a way as to provide for 5% degeneracy of base substitution at each of the residues (Hutchison *et al.*, 1991). Thus, a library of mutants of *rtp* was generated (Table II). In both

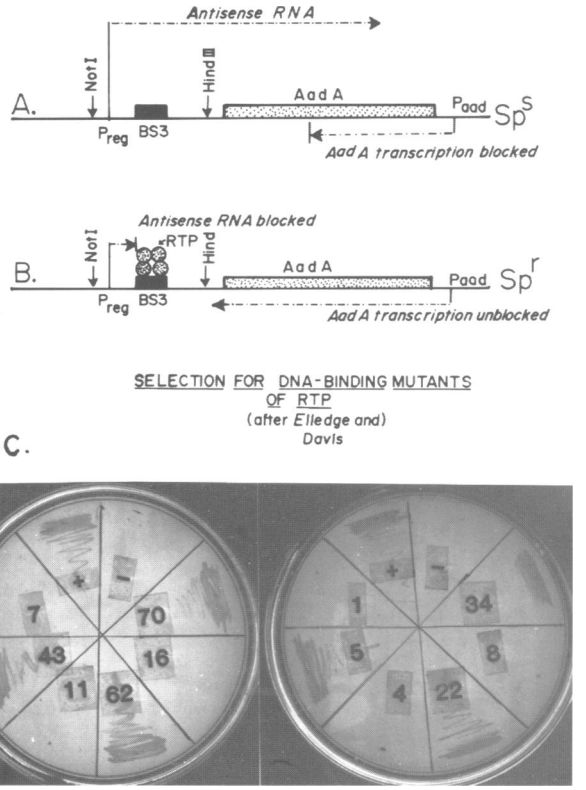

Fig. 2. The genetic selection (after Elledge *et al.*, 1989) for DNA-binding mutants of RTP. (**A**) In the *aadA* reporter plasmid, the expression of spectinomycin resistance is blocked by the antisense transcript initiated from the P_{reg} promoter. The cloned BS3 (IRI) site serves as a potential operator for the P_{reg} promoter. (**B**) In a cell milieu that contains normal RTP, the binding of the protein to the BS3 site turns off the antisense RNA, thus allowing the expression of the *aadA* gene and causing spectinomycin resistance (Sp^r). Mutant forms of RTP that are unable to bind to BS3 cause spectinomycin sensitivity (Sp^s). (**C**) Spectinomycin plates showing the response of various mutants of RTP: + indicates the presence of wild-type RTP in the cell; – indicates cells containing no RTP. Note that mutants 1, 4, 7, 8, 11 and 16 are potential DNA-binding mutants, whereas 5, 22, 34, 43, 62 and 70 show no defect in DNA binding, as confirmed by other tests described in the text.

cases, the selected mutants were characterized by DNA sequencing. Using the first scheme, we repeatedly selected the same mutations in codon 4 (E→K) and codon 8 (S→L) within the unstructured N-terminal arm. The second scheme generated a number of mutants defective in DNA binding, but these were also restricted to the N-terminal region of the protein. These mutants are 1, 7, 11 and 16 (Table II). Photographs of sample plates from the spectinomycin selection are shown in Figure 2C. The characteristics of the various single mutants with regard to their behavior on spectinomycin plates are listed in Table II.

These mutant proteins were expressed, purified and directly tested for their ability to specifically bind a 53 bp double-stranded DNA fragment containing the BS3 site. The fragment was end labeled with ^{32}P, incubated with various amounts of purified wild-type and mutant forms of RTP, and then analyzed on 6% non-denaturing polyacrylamide gels. Autoradiograms of the gels were quantitated as described. The experiments were also performed using a DNA fragment that contained only the core site of BS3 (data not shown). Quantitation of the binding data

Table I. Oligonucleotides used in mutagenesis and binding experiments

1.	RTP binding site used in the genetic selection scheme—top strand
	5′AATTCACTAAGAAAACTATGTACCAAATGTTCAGTCGAAATTTATTTTTTCCA3′
2.	Bottom strand
	5′AGCTTGGAAAAAATAAATTTCGACTGAACATTTGGTTACATAGTTTTCTTAGTG3′
Oligos used for mutagenesis	
3.	5′ATGAAAGAAGAAAAAAGGAGTTCAACAGGCTTTTTAGTG3′
4.	5′GTGAAACAGCGCGCATTTTTGAAGCTTTATATGATAACG3′
5.	5′ACGATGACAGAGCAAGAGAGACTCTATGGGTTAAAGCTG3′
6.	5′CTGCTTGAAGTACTTCGGTCTGAATTTAAAGAGATTGGT3′
7.	5′GGTTTTAAACCAAATCATACAGAAGTATACCGGTCTTTG3′
8.	5′TTGCATGAGCTTCTTGATGACGGGATACTAAAACAAATT3′
9.	5′ATTAAAGTAAAAAAAGAAGGGGCTAAGCTCCAGGAAGTC3′
10.	5′GTCGTCCTCTATCAATTTAAAGATTACGAAGCTGCCAAG3′
11.	5′AAGCTATATAAAAAACAGCTGAAGGTAGAGCTGGATCGC3′
12.	5′CGCTGTAAAAAACTGATTGAAAAAGCTCTCTCAGATAATTTTTAA3′
Oligos used for the incorporation of cysteine at specific points in *rtp* gene	
13.	E4C 5′ATGAAAGAATGTAAAAGGAGTTCAACA3′
14.	R16C 5′GTGAAACAGTGTGCATTTTTGAAG3′
15.	E56C 5′CCAAATCATACATGTGTATACCGGTCT3′
16.	R59C 5′GAAGTATACTGTTCTTTGCATG3′
17.	E63C 5′CGGTCTTTGCATTGTCTTCTTGATGAC3′
18.	K74C 5′AAACAAATTTGTGTAAAAAAGAAGGG3′

(shown in Figure 3, bottom, A) revealed that each of the mutant RTP proteins with changes in the N-terminal region is defective in DNA binding when compared to the wild-type protein. The R16G (RM16G) mutation showed the most severe defect (Figure 3, bottom, A). A number of mutants were recovered with changes in the β3 region (83, 84, 87, 88 and 89), but these showed the Sp^r phenotype, indicating no effect on DNA binding. This was confirmed by gel-shift experiments which gave the wild-type results (Table II).

Site-directed mutations based on the model of the RTP–DNA complex

The results of the random mutagenesis clearly show the importance of the unstructured N-terminal arm of RTP to DNA binding, which agrees well with our model. However, it has been shown by gel-shift experiments that the interaction requires two turns of DNA (Lewis *et al.*, 1990; Mehta *et al.*, 1992; Langley *et al.*, 1993) and must therefore involve more segments of the protein than simply the N-terminus. In particular, our model of the RTP–DNA complex specifically predicts that helix α3 and the β2/β3 ribbon are crucial DNA-binding elements. Although many mutants were obtained in the β3 strand which did not affect DNA binding, the random mutagenesis schemes failed to hit appropriate residues in the α3 helix and β2 strand. We therefore directly tested the model by rationally creating specific mutants (Table I) that would be predicted to disrupt DNA binding. In all cases, the wild-type amino acid was replaced by a cysteine residue to permit subsequent protein–DNA cross-linking studies on mutants found to be defective in binding DNA.

Mutants were tested both genetically and biochemically by the selection scheme and gel-shift experiments as described above. This approach proved to be very successful. Mutations generated within the α3 helix and the β2 strand regions of RTP were defective in DNA binding to varying degrees, as predicted by the model. Although the mutants showed reduced DNA binding, they still elicited the usual qualitative results in gel-shift experiments. Thus, using the BS3 site, one sees a double shift, α and β, caused by the occupation of the core and simultaneous occupation of both the core and the auxiliary sites, respectively (Figure 3, top). Cysteine substitutions at residues 56, 59 and 63 in the α3 helix caused a noticeable reduction in DNA binding, with the mutation at 59 showing the most dramatic effects (Figure 3, top and bottom, B). Although all of the mutations characterized above were either in the N-terminal unstructured arm or in the α3 helix, two of the mutations, namely R16G and K74C, were located in the α1 helix and the β2 strand, respectively.

The R16G mutation showed a noticeable reduction in DNA binding. It should be noted that although this mutation is located in the α1 helix, the folding of the protein brings it into close proximity with the α3 helix and thus makes R16 a *de facto* member of the latter.

Substitution at position 74 within the β2 strand showed no reduction in binding as determined by gel-shift assays (Figure 3, top and bottom, B), but it did yield the Sp^s phenotype in the *in vivo* assay (Table II), which indicated a defect in DNA binding. The characteristics of all of the site-directed mutants studies are shown in Table II.

Photo cross-linking of RTP–DNA complexes using cysteine derivatives

The cysteine-substituted mutant forms of RTP described above provided a convenient way of confirming their location at the RTP–DNA interface by photo cross-linking. Cysteines were also incorporated at residues 4 and 16 by

Table II. Mutants of RTP of *B.subtilis*

Codon	Base change	Amino acid change	Sp^s/Sp^r	DNA binding (+/–)	Contrahelicase activity (+/–)	Location
1	ATG→GTG	M→V	Sp^s	r	r	
4	GAA→AAA	E→K	Sp^s	r	r	
5	AAA→ATA	K→I	Sp^r	ND	ND	
7	AGT→AGG	S→R	Sp^s	r	r	N-terminal
8	TCA→TTA	S→L	Sp^s	r	r	
9	ACA→AGA	T→R	Sp^r	ND	ND	
11	TTT→TTG	F→L	Sp^s	r	r	
12	TTA→TTT	L→F	Sp^r	ND	ND	
16	CGC→GGC	R→G	Sp^s	r	r	
17	GCA→GAA	A→E	Sp^r	ND	ND	
19	TTG→TTC	L→F	Sp^r	+	ND	
22	TAT→TGT	Y→C	Sp^r	+	ND	α1
24	ATA→GTA	I→V	Sp^r	ND	ND	
25	ACG→GCG	T→A	Sp^r	ND	ND	
26	ATG→ATT	M→I	Sp^r	ND	ND	
27	ACA→CCA	T→P	Sp^r	ND	ND	
30	GAG→GGG	E→G	Sp^r	+	ND	
32	CTC→GTC	L→V	Sp^r	+	ND	
34	GGG→CGG	G→R	Sp^r	+	ND	β1
35	TTA→TTT	L→F	Sp^r	ND	ND	
36	AAG→GAG	K→E	Sp^r	ND	ND	
37	CTG→GTG	L→V	Sp^r	+	ND	
38	CTT→CCT	L→P	Sp^r	+	ND	α2
43	TCT→TAT	S→Y	Sp^r	ND	ND	
44	GAA→GTA	E→V	Sp^r	+	ND	
45	TTT→TTG	F→L	Sp^r	+	ND	
46	AAA→CCA	K→P	Sp^r	ND	ND	
47	GAG→GGG	E→G	Sp^r	+	ND	
49	GGT→TGT	G→C	Sp^r	+	ND	
50	TTT→ATT	F→I	Sp^r	ND	ND	
51	AAA→ATA	K→I	Sp^r	ND	ND	
52	CCA→CGA	P→R	Sp^r	ND	ND	
53	AAT→ACT	N→T	Sp^r	ND	ND	
55	ACA→GCA	T→A	Sp^r	ND	ND	
56	GAA→TGT	E→C	Sp^s	r	r	
58	TAC→TTC	Y→F	Sp^r	ND	ND	
59	CGG→TGT	R→C	Sp^s	r	r	
62	CAT→TAT	H→Y	Sp^r	ND	ND	α3
63	GAG→TGT	E→C	Sp^s	r	r	
64	CTT→GTT	L→V	Sp^r	ND	ND	
65	CTT→ATT	L→I	Sp^r	ND	ND	
66	GAT→GGT	D→G	Sp^r	ND	ND	
67	GAC→CAC	D→N	Sp^r	ND	ND	
68	GGG→CGG	G→R	Sp^r	ND	ND	
70	CTA→CGA	L→R	Sp^r	ND	ND	β2
74	AAA→TGT	K→C	Sp^s	+	r	
78	GAA→GGA	E→G	Sp^r	+	ND	
79	GGG→GTG	G→V	Sp^r	+	ND	
81	AAG→ATG	K→M	Sp^r	+	ND	Extended loop
83	CAG→CTG	Q→L	Sp^r	+	ND	
84	GAA→GTA	E→V	Sp^r	+	ND	
87	CTC→CAC	L→H	Sp^r	+	ND	β3
88	TAT→TTT	Y→F	Sp^r	+	ND	
89	CAA→CTA	Q→L	Sp^r	+	ND	
91	AAA→CAA	K→Q	Sp^r	ND	ND	
92	GAT→GTT	D→V	Sp^r	ND	ND	
96	GCC→GGC	A→G	Sp^r	ND	ND	
101	AAA→ACA	K→T	Sp^r	ND	ND	
102	CAG→CGG	Q→R	Sp^r	ND	ND	
104	AAG→ACG	K→T	Sp^r	ND	ND	
106	GAG→GTG	E→V	Sp^r	ND	ND	α4
109	CGC→CCC	R→P	Sp^r	ND	ND	
115	GAA→AAA	E→K	Sp^r	+	ND	
120	GAT→GAG	D→G	Sp^r	ND	ND	
121	AAT→AAA	N→K	Sp^r	ND	ND	
122	TTT→TGT	F→C	Sp^r	ND	ND	

ND, not determined.
r, reduced.

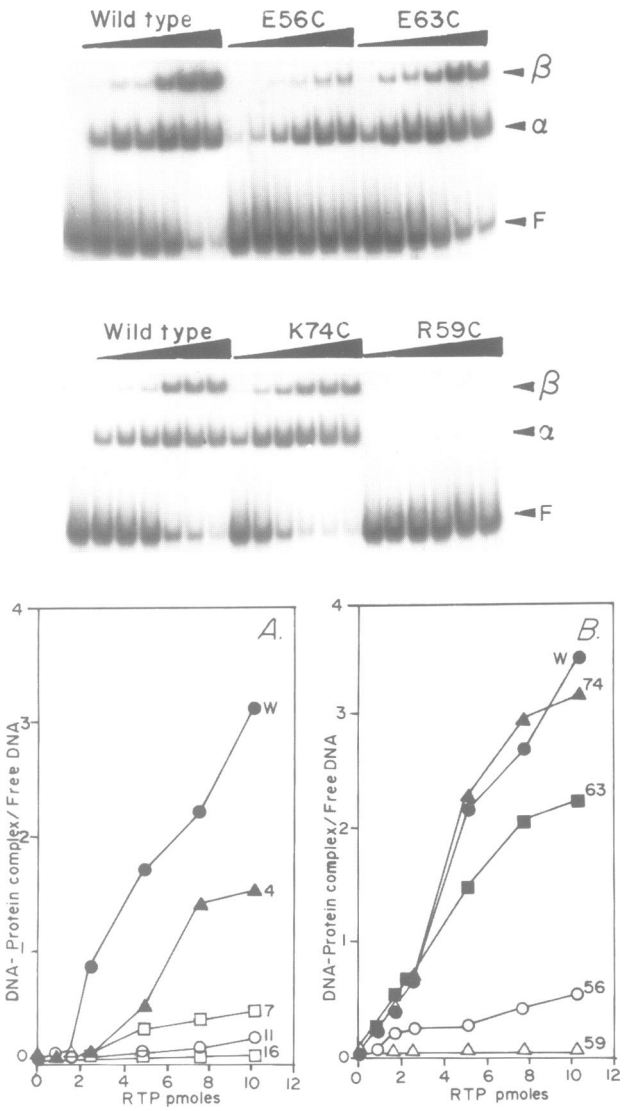

Fig. 3. Gel mobility shift assay for DNA binding. Top: autoradiogram showing mobility shift of a 53 bp labeled DNA fragment incubated with wild-type and various mutant forms of RTP. Qualitatively, mutant R59C shows the most noticeable loss of DNA binding, F, free DNA probe; α, shift caused by the occupation of the core site by RTP; β, shift caused by the occupation of both the core and the auxiliary sites. Bottom (**A** and **B**): binding curves of wild-type and various mutant forms of RTP. Both the BS3 DNA and separately a fragment containing just the core site were used and yielded identical results. Note that mutants 7, 11, 16, 56 and 59 show the most noticeable loss of DNA binding. Although mutant 74, located in the β2 strand, showed very little loss of DNA binding by this assay, functional analysis and photo cross-linking established that this amino acid was in contact with DNA in the termination complex.

site-directed mutagenesis (Table I) to confirm further the role of the N-terminal arm in DNA binding. These mutants are indicated by small, filled triangles in Figure 1A. Although the mutants are defective in binding DNA, they are each able to form a complex and would be expected to yield cross-linked species. The cysteines of each mutant were derivatized with azidophenacylbromide (Figure 4A) using the method of Pendergrast *et al.* (1992). RTP–DNA complexes were formed with end-labeled BS3 DNA, cross-linked by UV irradiation and finally visualized in 10% SDS–polyacrylamide gels. A naturally occurring cysteine at residue 110 on the opposite side of the protein

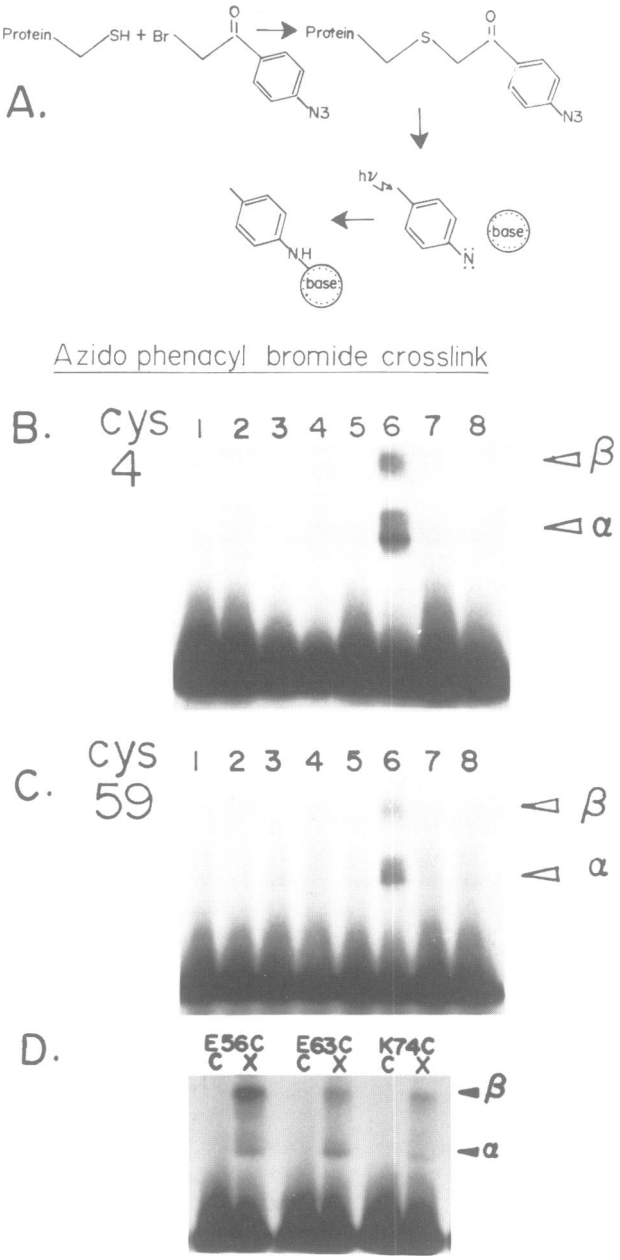

Fig. 4. Photo cross-linking of labeled BS3 DNA with normal and mutant forms of RTP at selected residues containing cysteine substitutions. (**A**) The derivatization of a cysteine residue with azidophenacylbromide (after Pendergrast *et al.*, 1992). (**B**) Autoradiogram of a SDS–polyacrylamide gel showing cross-linking of a mutant having cysteine at position 4. Lane 1, DNA probe without UV irradiation; 2, probe with UV irradiation; 3, wild-type RTP coupled at the natural cysteine residue at 110 and UV irradiated after being mixed with probe DNA; 4, probe + underivatized cys4 mutant protein; 5, derivatized cys4 protein + probe without UV; 6, derivatized cys4 protein + probe + UV irradiation (note the cross-linked α and β bands); 7 and 8, the same as lane 6, except that these also included 10- and 50-fold excess of homologous competitor, unlabeled DNA. (**C**) Lanes 1–8 are as in (B), except that the cys59 protein was used. (**D**) Photo cross-linking by mutant RTPs having cysteines at 56, 63 and 74; c, control, derivatized proteins + probe without UV; x, the same as c, except for UV irradiation. A full set of controls such as those shown in (B) and (C) was also performed for mutants 56, 63 and 74 (data not shown).

to the putative DNA-binding surface is buried within the coiled-coil dimerization domain in helix α4 and should not produce a cross-link. This was confirmed by performing the experiment with wild-type RTP (Figure 4B, lane 3). However, cysteine residues at positions 4, 16 (not shown), 56, 59, 63 and 74 specifically cross-linked to the DNA (Figure 4B–D), thus confirming that these amino acids either contact DNA or are within 11 Å of the DNA in the complex.

Contrahelicase activity of the mutant forms of RTP

The mutant proteins were individually purified and analyzed for the magnitude of their polar contrahelicase activity, i.e. their ability to block DnaB helicase of *E.coli* in the correct orientation of the terminus. The helicase assays showed that all of the mutants displayed some impairment of the polar activity. The mutations with the most noticeable loss of activity were residues 11 and 16 within the N-terminal arm (Figure 5A). Mutations at residues 56 and 59 within the α3 helix, and at residue 74 in the β2 strand, also showed a clear loss of activity (Figure 5B). Except in the case of mutant 74, the degree of impairment was inversely correlated with the avidity of DNA binding.

In vitro replication in the presence of the mutant forms of RTP

In a few selected cases, we measured the ability of the mutant forms of RTP to impede replication forks *in vitro*. We constructed two DNA templates called pUC-BS3 and pUC-BS3rev that contained the replication terminus in the functional and non-functional orientations, respectively, with respect to the replication origin. Cell extracts were made from *E.coli*, and the templates were replicated *in vitro* in the presence and absence of wild-type and various mutant forms of RTP in the reaction mixtures containing [α-^{32}P]dATP. The labeled reaction products were deproteinized and resolved in denaturing polyacrylamide gels. Since the terminus is located ~450 bp away from the origin, the successful arrest of the replication fork at the terminus should generate DNA strands some 450 nucleotides in length. As expected, the wild-type RTP arrested the replication forks at the terminus in the pUC-BS3 template (Figure 6, lanes 2–5), but no arrest was visible on the pUC-BS3rev template (data not shown). In contrast, mutants 16, 59 and 74 did not arrest replication forks *in vitro* on either of the templates (Figure 6, lanes 6–17; data for pUC-BS3rev not shown). Thus, the failure of the mutant forms of RTP to arrest replication was directly correlated with their DNA-binding activities.

Crystallography of the RTP mutant R16G (RM16G)

A concern with mutagenesis studies is whether the mutation is truly modifying the protein's function or simply disrupting its three-dimensional structure. Since the site-directed mutants all involve surface residues, as shown by the crystal structure, we are confident that their structures are unchanged, and this is supported by their behavior in solution, which is indistinguishable from that of the wild type. The mutants derived from genetic selection are more problematic. Residues 4 and 8 are within the disordered N-terminal arm and are unlikely to affect the overall structure, but the arginine to glycine mutation at

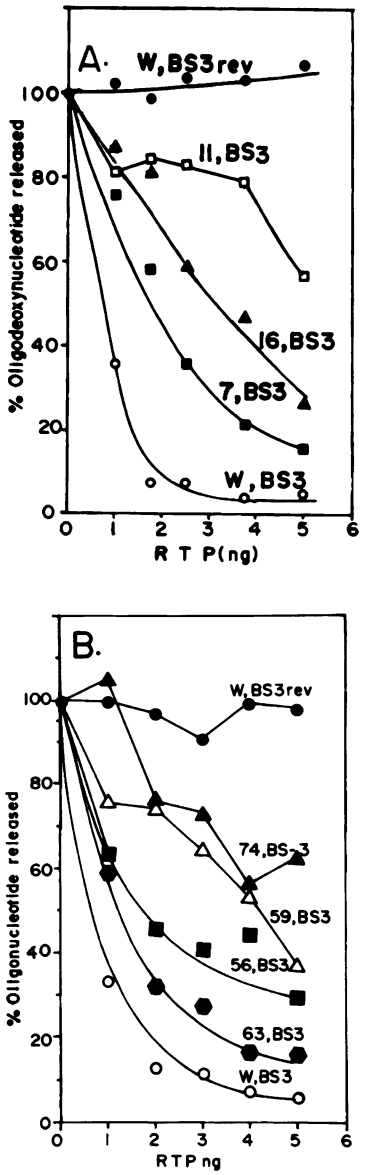

Fig. 5. Contrahelicase activities of wild-type and mutant forms of RTP. As expected, the wild-type RTP blocked DnaB helicase on the BS3 substrate, but not on the BS3rev substrate. The mutants were unable to block DnaB activity on the BS3rev substrates (data not shown). Note the different magnitude of impairment of contrahelicase activity in the various DNA-binding mutants of RTP. Note that mutant 74, located in the β2 strand, shows ~50% loss of activity in comparison with the wild-type protein on the BS3 substrate.

position 16 could potentially introduce disrupting flexibility. We therefore decided to solve its crystal structure.

The mutant protein crystallized in the same space group and with the same unit cell dimensions as the wild-type protein (space group C2; a = 76.7 Å, b = 52.4 Å and c = 70.4 Å and β = 90°). Diffraction data were collected to 2.6 Å and the mutant structure was refined and carefully analyzed by difference Fourier maps. The mutant structure deviated very little from that of the wild type. The RMS deviation between the α-carbons of the mutant and the wild-type structure is 0.66 Å (residues 7–122), and a superposition of the α-carbon backbones is shown in Figure 7A. The only significant changes are at the N-terminus and in the loop between residues 78 and 82.

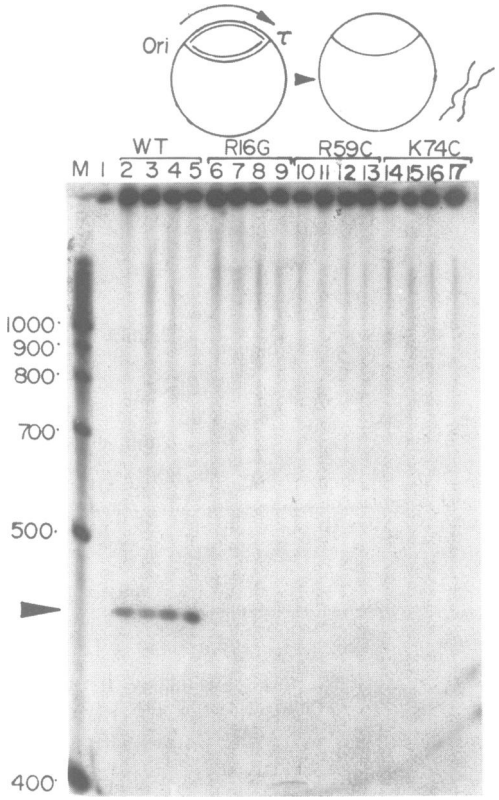

Fig. 6. Ability of wild-type and various mutant forms of the protein to terminate DNA replication *in vitro*. Top: Schematic representation of the procedure used for detecting fork arrest. Since the terminus (τ) is located ~450 bp from the origin (ori), denaturation of arrested intermediates should generate ~450 nucleotide long strands. Bottom: Autoradiogram of a 6% denaturing polyacrylamide gel showing the products of *in vitro* replication reactions. Lane M, molecular size markers; lane 1, control extract without RTP; lanes 2–5, replication products of the plasmid pUC18-BS3 in the presence of 50, 100, 150 and 200 ng of normal RTP; lanes 6–9, the same as in lanes 2–5, except that R16G RTP was used; lanes 10–13, same as in lanes 6–9, respectively, except that R59C RTP was used; lanes 14–17, the same as in the lanes 2–5, respectively, except that K74C RTP was used. The pUC19-BS3rev template was used as a control and, as expected, failed to arrest replication forks at the terminus (data not shown). The arrow indicates the ~450 bp arrested band characteristic of replication fork arrest at τ.

However, since the electron density in these regions is weak, they appear to have considerable inherent flexibility (Bussiere *et al.*, 1995).

Discussion

Although the crystal structure of RTP has been solved and certain predictions regarding the DNA-binding domain of RTP have been made, direct experimental proof for the proposed RTP–DNA interaction was not available (Bussiere *et al.*, 1995). Taken together, the various data described in this paper, using a variety of experimental approaches, provide convincing evidence that our model is basically correct and also allow further refinements to it. Thus, the data show that the unstructured N-terminal arm, the α3 helix and the β2 strand are either making a direct contact with the terminus DNA or are located within 11 Å of the DNA (Figure 7B). A prediction from the model was that the N-terminal arm, which is not visible in the structure, is flexible and could wrap around the DNA and make non-specific but important ionic interactions with the DNA. Such a role is clearly supported by the mutagenesis results and is reminiscent of similar unstructured regions in other DNA-binding proteins. For example, the N-terminal arms of the lambda repressor (Pabo *et al.*, 1982) and the Msx homeodomain (Shang *et al.*, 1994) are known to contribute to the high-affinity binding and to stabilize the protein–DNA complex. It would be reasonable to expect that the N-terminal arm of RTP performs a similar function. The results from two of the mutagenized residues deserve some additional discussion since they provide a fine tuning of the model.

Arginine 16 is formally located within helix α1 and is not within one of the three DNA-binding secondary structure elements. However, examination of the RTP structure shows that this extended side chain is positioned in such a way as to become a *de facto* member of the α3 helix. The γ-carbon of arginine 16 is only some 6.0 Å away from the γ-carbon of arginine 59 and is within 4.3 Å of the δ-carbon of glutamate 63 (both within α3). This location positions arginine 16 for contact either with the phosphate backbone or with bases in the major groove. Substitution by a glycine at this position could disrupt

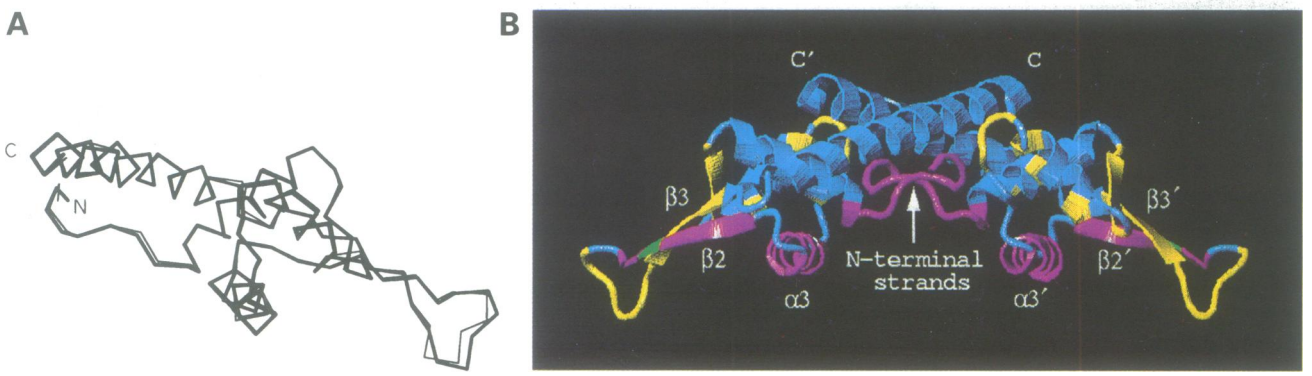

Fig. 7. The tertiary structures of wild-type and the R16G mutant RTP and the 'winged helix' DNA-binding domain. (**A**) Superimposition of the α-carbon backbone structures of the wild-type (thick line) and the mutant form (thin line) of RTP. Note that there are no significant differences in the two structures. (**B**) Tertiary structure of RTP (Bussiere *et al.*, 1995) showing the locations of the regions of the protein that either contact DNA or are located within 11 Å of the terminus DNA. The evidence presented in this paper is consistent with the conclusion that the N-terminal arm, the α3 helix and the β2 strand are the DNA-binding regions (crimson). Regions that do not affect DNA binding are in yellow. The green region within strand β2 is the location of lysine 74, which reduces DNA binding *in vivo*, causes partial loss of contrahelicase activity and complete loss of replication fork arrest activity. Note the β2, β3 and the extended loop connecting the two form the wings of the winged helix.

DNA binding either by reducing the overall electrostatic binding energy or by affecting specific DNA recognition.

The mutation of lysine 74 to cysteine resulted in no obvious change in the DNA-binding activity of RTP when examined by the gel mobility shift assay (Figure 3, top and bottom, B), but the obviously subtle effect on DNA binding is shown by the genetic selection assay (Table II). The positive result from the the photo cross-linking experiment using mutant K74C confirms that the β2 strand is in close proximity to the bound DNA (Figure 4D). Examination of the β2 sequence reveals four lysine residues (71, 74, 76 and 77) which suggests that its interaction with DNA is predominantly non-specific and electrostatic (Figure 7B). The removal of the single lysine 74 would be predicted to have a minimal effect on the DNA binding. Positively charged residues along one strand of a DNA-binding ribbon that binds the DNA minor groove are also seen in the HU structure (White *et al.*, 1988; Yang and Nash, 1989). Our original model for the RTP–DNA complex proposed that the complete β2/β3 ribbon would interact with DNA, but none of the mutants in the β3 strand showed DNA-binding defects (Table II). Recent results from our laboratory indicate that β3 is involved in the RTP-RTP cooperative interaction (Manna *et al.*, 1996).

The most direct evidence that the three structural features of RTP participate in DNA binding came from the cross-linking analyses using the site-specific cysteine mutants (Figure 4). Unfortunately, although the azidophenacylbromide procedure yielded amino acid-specific cross-links, we were unable to map the DNA elements contacted by the amino acids because the DNA chain could not be cleaved at the cross-linked site by alkali treatment (Pendergrast *et al.*, 1992). We attempted to map the sites by a variety of other procedures, including hydroxy radical cleavage of the cross-linked DNA, but were unsuccessful in our efforts. We are in the process of using Fe-EDTA coupling (Mazzarelli *et al.*, 1993) and copper *o*-phenanthroline (Ebright *et al.*, 1990; Pan *et al.*, 1994) to convert the RTP to a chemical nuclease, and have begun to systematically map the important protein–DNA contacts.

An important consideration throughout this analysis has been the biological function of RTP and how this is affected by the various mutations. Our models for how RTP operates all require that it binds firmly and specifically to its cognate DNA, and any disruption of this interaction should elicit effects on contrahelicase activity and replication termination. The DNA-binding domain almost certainly plays a critical role in the termination process not only by presenting the helicase to the RTP bound at the termination site, but also as an important determinant of the polarity of the process (Sahoo *et al.*, 1995a). It is clear from Table II that this is indeed the case. The only exception of any significance is mutant K74C which showed a clear decline in contrahelicase activity (Figure 5B) and in the ability to arrest replication forks at the BS3 site (Figure 6, lanes, 14–17), but which showed wild-type DNA binding on gel-shift assays (Figure 3, top and bottom, B). However, a subtle effect on DNA binding was apparent in the genetic selection experiments (Table II). A second consideration was the structural integrity of the mutant proteins to ensure that any DNA-binding defects are not simply the result of protein deformations. This was verified by crystallographic analysis for mutant R16G where this was a potential problem (Figure 7A). All the remaining mutants affect surface amino acids that contribute little to the protein's stability.

It was recently noted that RTP is a member of the so-called 'winged helix' family of DNA-binding proteins (Swindells, 1995). This family, which includes the Fork Head transcription factor (Clark *et al.*, 1993), Lex A (Fogh *et al.*, 1994) and histone H5 (Ramakrishnan *et al.*, 1993), bind DNA via an α helix and an adjacent β strand at successive major and minor grooves. We predicted such a model for RTP without noticing the homology (Bussiere *et al.*, 1995), but the homology has now allowed a better model to be constructed in which the DNA is slightly bent (Swindells, 1995). The data presented in this paper are fully consistent with this revised model (Figure 7B), and we also have preliminary data to indicate that RTP does cause a modest amount of DNA bending *in vitro* (unpublished data). We are presently attempting to grow crystals of the RTP–DNA complex to view the interaction directly.

Material and methods

Bacterial strains and plasmids

Escherichia coli JM109 [*sup44 relA1 recA1 endA1 gyrA96 thi hsdR17* Δ(*lac-ProAB*) F′(*traD36 lacZ M15 proAB*)] was used as the host in all of the transformation and mutagenesis work. The *rtp* gene was cloned into M13mp18 as an *Xba*I–*Bam*HI fragment and used for the synthesis of uracil-containing ssDNA from CJ236 (F′ *cat/dut ung1 thi-1 relA1 spoT1 mcrA*). *Escherichia coli* BL21 DE3 (plysS) cells were used for overexpressing normal and mutagenized *rtp* gene cloned in a T7 expressing system. Plasmids pNN396 and pNN388 used in the genetic selection scheme were obtained from R.W.Davis. Drugs, ampicillin (50 mg/ml), chloramphenicol (40 mg/ml), kanamycin (50 mg/ml) and spectinomycin (80 mg/ml) were used where necessary.

Purification of proteins

Mutagenized *rtp* gene from M13mp18 was cloned into pET13A as a *Xba*I–*Bam*HI fragment and transformed into BL21 plysS. Wild-type and mutant RTP proteins were purified as described earlier (Mehta *et al.*, 1992). DnaB was purified using a published procedure (Khatri *et al.*, 1989).

Random chemical mutagenesis

Hydroxylamine was used to mutagenize *rtp* gene cloned in pET13A at *Nde*I–*Bam*HI restriction sites. The recombinant DNA containing *rtp* gene was incubated with 1 M hydroxylamine (pH 7.0) for 24 h at 37°C. The reaction was stopped by the addition of 5 M NaCl, bovine serum albumin (1 mg/ml) and ethanol. Earlier experiments showed that transformation of recombinant *rtp* DNA treated with 1 M hydroxylamine for 24 h resulted in survival of only 10–15% of colonies compared with the untreated control DNA. Mutagenized *rtp* gene was taken out as an *Nde*I–*Bam*HI cassette, cloned into unmutagenized vector and transformed into CJ236 cells. The colonies were pooled, DNA was prepared and screened through the genetic selection scheme (Figure 2) to identify mutants defective in DNA binding. Approximately 3000 colonies were examined and the DNAs from spectinomycin- and kanamycin-sensitive (Sp^sKm^s) colonies were sequenced for the possible mutations. Only eight mutants were identified, of which five contained mutation in codon 8, while the remaining three had mutations in codon 4 (Table II).

Saturation mutagenesis

Since hydroxylamine is known only to react with cytosine, we decided to carry out saturation mutagenesis of *rtp* gene, isolate mutants and screen them through the genetic selection scheme so that we would be able to identify additional mutants defective in DNA binding, which were not obtained by chemical mutagenesis. Ten overlapping oligonucleotides were designed (Table I) and a 5% degeneracy of bases was allowed at each step of synthesis to enable us to isolate a large range of base pair

substitutions. Mutagenesis was carried out as described by Hutchison *et al.* (1991). Briefly, mutagenized oligonucleotides were kinased using 10 mM ATP and T4 polynucleotide kinase, and 0.2 pmol of the kinased oligonucleotides were annealed to 0.8 pmol of uracil-containing single-stranded M13mp18-*rtp* DNA in a water bath at 65°C for 15 min and the water was cooled to room temperature. Hybridized oligonucleotides were extended in a reaction volume of 100 µl containing 0.5 mM dNTPs, 10 mM $MgCl_2$, 20 mM dithiothreitol, 20 mM HEPES pH 7.8, 2.5 U T4 DNA polymerase and 2 U T4 DNA ligase at 37°C for 2 h. The reactions were stopped by the addition of 0.5 M EDTA. The reaction mixtures were transformed in JM109 and the plaques were pooled to obtain a library of mutants. The mutants were identified by dideoxy sequencing reaction (US Biochemicals) and were screened through the genetic selection scheme to identify the DNA-binding defect (Table II).

Genetic selection scheme

The transcriptional interference assay used in this study was adapted from earlier work of Elledge *et al.* (1989). RTP binding site BS3 (53 bp) was blunt ended by Klenow DNA polymerase and cloned into the *Sma*I restriction site of pNN396. The *Not*I–*Hin*dIII cassette, from pNN396 containing the P_{reg} promotor and the RTP binding site (operator), in both orientations, was cloned into the plasmid pNN388. In pNN388, the *aadA* (aminoglycoside 3′-adenyl transferase) gene required for the hydrolysis of spectinomycin is normally expressed, conferring resistance to the drug (Sp^r). However, insertion of the P_{reg} promoter and the operator (together P_{reg}) represses the transcriptional expression of *aadA* gene conferring spectinomycin sensitivity (Sp^s), in the absence of RTP. RTP binds to the operator site following co-transformation with pET13A (has kanamycin marker) containing the *rtp* gene, causing suppression of the antisense transcript. The transcript of *aadA* is thus allowed to be expressed, thus conferring on the cells spectinomycin resistance (Sp^r) and kanamycin resistance (Km^r, carried by the pET13A vector). Mutants isolated by saturation mutagenesis were screened using this selection system and those defective in DNA binding (Sp^sKm^s) were identified (Table II). Similarly, the genetic selection system was also used to isolate DNA-binding defect mutants following chemical mutagenesis.

Gel mobility shift assay

Gel mobility shift assays were carried out as described previously (Mehta *et al.*, 1992; Sahoo *et al.*, 1995a). In brief, RTP binding site (BS3) was end-labeled using [γ-^{32}P]ATP and T4 polynucleotide kinase, and mixed with the reaction buffer (20 µl) containing 20 mM Tris–HCl pH 7.4, 50 mM potassium glutamate, 10% glycerol, 1 mg bovine serum albumin and 7.5 µg calf thymus DNA. Various concentrations (0–300 ng) of wild-type and mutant RTPs were added to the reaction mixtures and incubated at room temperature for 30 min. The reaction mixtures were resolved on a 6–8% polyacrylamide gel and scanned through a phosphorimager.

Azidophenacylbromide-mediated photo cross-linking

Coupling of the azidophenacyl moiety to wild-type RTP and cysteine-substituted mutants was carried out as described previously (Pendergrast *et al.*, 1992). Briefly, 100 µg of protein were added to the total reaction mixture (500 µl) containing 300 mM azidophenacylbromide, 20 mM Tris–HCl pH 8.0, 200 mM KCl, 0.1 mM EDTA, 5% (v/v) glycerol and 1.7% dimethyl formamide. Incubations were carried out in the dark for 3 h, followed by 15 h at 4°C. Reaction mixtures were dialyzed against 20 mM Tris–HCl pH 8.0, 0.1 mM EDTA, 50 mM KCl and 10% (v/v) glycerol for 3 h in the dark at 4°C to remove unreacted reagent and stored in aliquots at –20°C. Ellman's reagent was used to monitor the efficiency of coupling. Wild-type RTP contained one, while mutant proteins had two moles of solvent-accessible cysteines per mole of protein. Following coupling, products contained <20% solvent-accessible cysteines.

UV cross-linking of azido-coupled proteins were carried out as follows. The reaction mixture (50 µl) contained 50–100 ng of coupled proteins, 0.1 pmol of ATP 5′-end-labeled RTP binding site (BS3) DNA, 10 mM MOPS–NaOH pH 7.3, 200 mM NaCl and 50 µg bovine serum albumin per milliliter. Reaction mixtures were incubated at room temperature in the dark for 45 min. UV irradiation of mixtures was carried out from a distance of 10 cm for 2 min at room temperature using a UV hand lamp (Model UVGL-25; Ultraviolet Products, San Gabriel, CA). UV-irradiated mixtures were resolved on a SDS–10% polyacrylamide gel.

Helicase assay

Helicase assays were carried out as described previously (Khatri *et al.*, 1989).

In vitro replication

In vitro replication assays were carried out as described previously (Ruiz-Echevaria *et al.*, 1995). The products were deproteinized by proteinase K digestion and analyzed in denaturing polyacrylamide gels.

X-ray crystallographic studies of mutant R16G

The crystals of mutant R16G were grown in 20% PEG 2000 (w/v) buffered with 0.125 M MES pH 6 as described previously (Mehta *et al.*, 1992). The mutant form of the protein crystallized in the same space group and with the same unit cell dimensions as the wild-type protein (space group C2; a = 76.7 Å, b = 52.7 Å, c = 70.4 Å, β = 90°; two monomers in the asymmetric unit). Diffraction data were collected as described previously (Bussiere *et al.*, 1995), and were processed and reduced using DENZO (Otwinoski, 1993). The final data set was 84% complete to 2.6 Å, and the overall R_{merge} for the 8827 unique reflections (24 607 total) was 3.9%.

An atomic model was constructed from the native structure (Bussiere *et al.*, 1995) which incorporated the R16G mutation, and it comprised both of the independent monomers in the unit cell. This model was refined against the R16G data using the program X-PLOR (Brünger, 1988). Only data within the range of 10–2.6 Å and above a 2 sigma cut-off were used in the refinement. The refinement protocol consisted of 200 steps of Powell minimization, one round of simulated annealing using initial and final temperatures of 3000 and 300°K, respectively, and 20 cycles of individual restrained B factor refinement. Each monomer was treated independently during the refinement process, and full electrostatic calculations with the standard cut-off were included at each step. The structures of the monomers were examined with the O program (Jones *et al.*, 1991) using a combination of ($2F_o$–F_c), (F_o–F_c) and ($2F_o$–F_c) 'omit' maps. In the latter, residue 16 was omitted from all calculations to confirm the correct placement of the residue in the electron density map. The R factor fell from an initial value of 27.6% to a final value of 21.2% following the completion of refinement. The atomic model has an RMS deviation of 0.024% in bond lengths and 4.24° in bond angles.

Acknowledgements

We thank Susan Almore for synthesizing some of the oligonucleotides. This work was supported by grants GM 49264 to D.B and S.W.W, the Merit award R37AI19881 to D.B and also by a grant AI 08989 from the NIH to C.A.H.

References

Bastia,D., Germino,J., Crosa,J.H. and Ram,J. (1981) The nucleotide sequence surrounding the replication terminus of R6K. *Proc. Natl Acad. Sci. USA*, **72**, 2095–2099.

Brunger,A.T. (1988) *X-PLOR: A System for X-Ray Crystallography and NMR*. Yale University Press, New Haven, CT.

Bussiere,D.E., Bastia,D. and White,S.W. (1995) Crystal structure of the replication terminator protein from *B. subtilis* at 2.6Å. *Cell*, **80**, 651–660.

Carrigan,C.M., Pack,R.A., Smith,M.T. and Wake,R.G. (1991) Normal terC-region of *Bacillus subtilis* chromosome acts in a polar manner to arrest the clockwise replication fork. *J. Mol. Biol.*, **222**, 197–207.

Clark,K.L., Halay,E.D., Lai, E. and Burley,S. (1993) Co-crystal structure of the HNF-3/*fork head* DNA-recognition motif resembles histone H5. *Nature*, **364**, 412–420.

Ebright,R.H., Ebright,Y.W., Pendergrast,P.S. and Gunasekera,A. (1990) Conversion of a helix-turn-helix motif sequence-specific DNA binding protein into a site-specific DNA cleavage agent. *Proc. Natl Acad. Sci. USA*, **87**, 2882–2886.

Elledge,S.J., Sugino,P., Guarente,L. and Davis,R.W. (1989) Genetic selection for genes encoding sequence-specific DNA-binding proteins. *Proc. Natl Acad. Sci. USA*, **86**, 3689–3693.

Fogh,R.H., Ottleben,G., Ruterjans,H., Schnarr,M., Boelens,R. and Kaptein,R. (1994) Solution structure of the LexA repressor DNA binding domain determined by NMR spectroscopy. *EMBO J.*, **13**, 3936–3944.

Hiasa,H. and Marians,K.J. (1992) Differential inhibition of the DNA translocation and DNA unwinding activities of DNA helices by *Escherichia coli* Tus protein. *J. Biol. Chem.*, **267**, 11379–11385.

Hill,T.M., Tecklenburg,M., Pelletier,A.J. and Kuempel,P.L. (1989) tus, the trans-acting gene required for termination of DNA replication in *Escherichia coli*, encodes a DNA binding protein. *Proc. Natl Acad. Sci. USA*, **86**, 1593–1597.

Hutchison,C.A., Swanstrom,R. and Loeb,D.D. (1991) Complete mutagenesis of protein coding domains. *Methods Enzymol.*, **202**, 356–390.

Jones,T.A., Zou,J.Y., Cowan,S.W. and Kjeldgaard,M. (1991) Improved methods for building protein molecules in electron density maps and the location of errors in these models. *Acta Crystallogr.*, **A47**, 110–119.

Kaul,S., Mohanty,B.K., Sahoo,T., Patel,I., Khan,S.A. and Bastia,D. (1994) The replication terminator protein of the gram positive bacterium *B. Subtilis* functions as a polar contrahelicase in gram negative *E. coli*. *Proc. Natl Acad. Sci. USA*, **91**, 11143–11147.

Khatri,G.S., MacAllister,T., Sista,P.R. and Bastia,D. (1989) The replication terminator protein of *E. coli* is a DNA sequence-specific contra-helicase. *Cell*, **59**, 667–674.

Kolter,R. and Helinski,D. (1978) Activity of the replication terminus of plasmid R6K in hybrid replicons in *Escherichia coli*. *J. Mol. Biol.*, **124**, 425–441.

Kuempel,P.L., Duerr,S.A. and Seeley,N.R. (1977) Terminus region of the chromosome in *Escherichia coli* inhibits replication forks. *Proc. Natl Acad. Sci. USA*, **72**, 2095–2099.

Langley,D.B., Smith,M.T., Lewis,P.J. and Wake,R.G. (1993) Protein-nucleoside contacts in the interaction between the replication terminator protein of *Bacillus subtilis* and the DNA terminator. *Mol. Microbiol.*, **10**, 771–779.

Lee,E.H., Kornberg,A., Hidaka,M., Kobayashi,J. and Horiuchi,T. (1989) *Escherichia coli* replication termination protein impedes the action of helicases. *Proc. Natl Acad. Sci. USA*, **86**, 9104–9108.

Lewis,P.J. and Wake,R.G. (1989) DNA and protein sequence conservation at the replication terminus in *Bacillus subtilis* 168 and W23. *J. Bacteriol.*, **171**, 1402–1408.

Lewis,P.J., Smith,M.T. and Wake,R.G. (1989) A protein involved in the termination of chromosome replication in *Bacillus subtilis* binds specifically to the terC site. *J. Bacteriol.*, **171**, 3564–3567.

Lewis,P.J., Ralston,G.B., Christopherson,R.I. and Wake,R.G. (1990) Identification of the replication terminator protein binding sites in the terminus regions of the *Bacillus subtilis* chromosome and the stoichiometry of binding. *J. Mol. Biol.*, **214**, 73–84.

Louarn,J., Patte,J. and Louarn,J.M. (1977) Evidence for a fixed termination site of chromosome replication in *Escherichia coli* K12. *J. Mol. Biol.*, **115**, 295–314.

Manna,A.C., Pai,K.S., Bussiere,D.E., White,S.W. and Bastia,D. (1996) The dimer-dimer interaction surface of the replication terminator protein of *Bacillus subtilis* and termination of DNA replication. *Proc. Natl Acad. Sci. USA*, **93**, 3253–3258.

Mazzarelli,J.M., Ermacora,M.R., Fox,R.O. and Grindley,N.D.F. (1993) Mapping interactions between the catalytic domain of resolvase and its DNA substrate using cysteine-coupled EDTA-iron. *Biochemistry*, **32**, 2979–2986.

Mehta,P.P., Bussiere,D.E., Hoffman,D.W., Bastia,D. and White,S.W. (1992) Crystallization and preliminary structural analysis of the replication terminator protein *Bacillus subtilis*. *J. Biol. Chem.*, **267**, 18885–18889.

Otwinoski,Z. (1993) Oscillation data reduction program. Data collection and processing. In Sawyer,L., Isaacs,N. and Bailey,S. (eds), *Proceedings of the CCP4 Study Weekend*. SERC Daresbury Lab, UK, pp. 56–62.

Pabo,C.O., Krovatin,K., Jeffrey,A. and Sauer,R.T. (1982) The N-terminal arms of lambda repressor wrap around the operator DNA. *Nature*, **298**, 441–443.

Pan,C.Q., Feng,J.A., Finkel,S.E., Laudraf,R., Sigman,D. and Johnson,R.C. (1994) Structure of the *Escherichia coli* Fis-DNA complex probed by protein conjugated with 1,10-phenanthroline copper(I) complex. *Proc. Natl Acad. Sci. USA*, **91**, 1721–1725.

Pendergrast,P.S., Chen,Y., Ebright,Y.W. and Ebright,R.H. (1992) Determination of the orientation of a DNA binding motif in a protein–DNA complex by photocrosslinking. *Proc. Natl Acad. Sci. USA*, **89**, 10287–10291.

Ramakrishnan,V., Finch,J.T., Graziano,V., Lee,P.L. and Sweet,R.M. (1993) Crystal structure of globular domain of histone H5 and its implications for nucleosome binding. *Nature*, **362**, 219–223.

Ruiz-Echevarria,M.J., Gimenez-Gallego,G., Sabariegos-Jareno,R. and Diaz-Orejas,R. (1995) Kid, a small protein of the parD stability system of plasmid R1, is an inhibitor of DNA replication acting at the intiation of DNA synthesis. *J. Mol. Biol.*, **247**, 568–577.

Sahoo,T., Mohanty,B.K., Patel,I. and Bastia,D. (1995a) Termination of DNA replication *in vitro*: requirement for stereospecific interaction between two dimers of the replication terminator protein of *Bacillus subtilis* and with terminator site to elicit polar contrahelicase and fork impedance. *EMBO J.*, **14**, 619–628.

Sahoo,T., Mohanty,B.K., Lobert,M., Manna,A.C. and Bastia,D. (1995b) The contrahelicase activities of the replication terminator proteins of *Escherichia coli* and *Bacillus subtilis* are helicase-specific and impede both helicase translocation and authentic DNA unwinding. *J. Biol. Chem.*, **270**, 29138–29144.

Shang,Z., Issac,V.E., Li,H., Patel,L., Catron,K.M., Curran,T., Montelione,G.T. and Abate,C. (1994) Design of a 'minimA1' homeodomain: The N-terminal arm modulates DNA binding affinity and stabilizes homeodomain structure. *Proc. Natl Acad. Sci. USA*, **91**, 8373–8377.

Sista,P.R., Mukharjee,S., Patel,P., Khatri,G.S. and Bastia,D. (1989) A host-encoded DNA-binding protein promotes termination of plasmid replication at a sequence-specific replication terminus. *Proc. Natl Acad. Sci. USA*, **86**, 3026–3030.

Smith,M.T. and Wake,R.G. (1992) Definition and polarity of action of DNA replication terminators in *Bacillus subtilis*. *J. Mol. Biol.*, **227**, 648–657.

Swindells,M.B. (1995) Identification of a common fold in the replication terminator protein suggests a possible mode of DNA binding. *Trends. Biochem. Sci.*, **20**, 300–302.

White,S.W., Appelt,K., Wilson,K.S. and Tanaka,I. (1988) A protein structural motif that bends DNA. *Proteins: Struct. Funct. Genet.*, **5**, 281–288.

Yang,C.-C. and Nash,H.A. (1989) The interaction of *E.coli* IHF protein with its specific binding sites. *Cell*, **57**, 869–880.

Young,P.A. and Wake,R.G. (1994) The *Bacillus subtilis* replication terminator system functions in *Escherichia coli*. *J. Mol. Biol.*, **240**, 275–280.

Received on December 11, 1995; revised on February 9, 1996